Dumortierite from the Gföhl unit, Lower Austria: Chemistry, structure, and infra-red spectroscopy

Article *in* European Journal of Mineralogy · March 2005

DOI: 10.1127/0935-1221/2005/0017-0173

Eur. J. Mineral.
2005, **17**, 173-183

Dumortierite from the Gföhl unit, Lower Austria: chemistry, structure, and infra-red spectroscopy

YVES FUCHS[1,*], ANDREAS ERTL[2], JOHN M. HUGHES[3], STEFAN PROWATKE[4], FRANZ BRANDSTÄTTER[5] and RALF SCHUSTER[6]

[1]Laboratoire des Géomatériaux, FRE 2455 CNRS, Université de Marne La Vallée, 5 Bd Descartes, Champs sur Marne, F-77454 Marne La Vallée Cedex 2, France
[2]Institut für Mineralogie und Kristallographie, Geozentrum, Universität Wien, Althanstraße 14, A-1090 Wien, Austria
[3]Department of Geology, Miami University, Oxford, Ohio 45056, U.S.A.
[4]Mineralogisches Institut, Universität Heidelberg, Im Neuenheimer Feld 236, D-69120 Heidelberg, Germany
[5]Mineralogisch-Petrographische Abteilung, Naturhistorisches Museum, A-1014 Wien, Austria
[6]Geologische Bundesanstalt, Rasumovskigasse 23, A-1030 Wien, Austria

Abstract: For dumortierite from Gföhl, Lower Austria, crystal structure refinement in combination with chemical analyses gives the optimized formula $(Al_{0.78}\square_{0.12}Mg_{0.09}Ti_{0.01})$ $(Al_{5.70}\square_{0.20}Ti_{0.06}Fe_{0.04})$ $(Si_{2.85}Al_{0.15})$ B O_{16} $[O_{1.17}(OH)_{0.81}F_{0.02}]$, with $a = 4.6900(3)$, $b = 11.7875(6)$, $c = 20.1823(11)$ Å. For dumortierite from Weißenkirchen in der Wachau, Lower Austria, crystal structure refinement in combination with the chemical analyses gives the optimized formula $(Al_{0.74}\square_{0.13}Mg_{0.12}Ti_{0.01})$ $(Al_{5.70}\square_{0.20}Ti_{0.08}Fe_{0.02})$ $(Si_{2.83}Al_{0.17})$ B O_{16} $[O_{1.14}(OH)_{0.85}F_{0.01}]$, with $a = 4.6948(2)$, $b = 11.8037(5)$, $c = 20.2106(8)$ Å. Complete chemical characterizations, including light elements (B, H, Li, Be), were combined for the first time with high-quality structure refinements with *R*-values in the range 0.018-0.019, allowing assignment of site-occupancies with confidence. The optimizations demonstrate that all Mg occupies the *M*1 sites. Mg substitution at *M*1 plays a prevailing role in the high number of absorption bands. Contrary to *M*2, *M*3 and *M*4, the *M*1 site has substantial vacancies. Whereas the average *M*-O distances of the *M*2 and *M*3 sites are similar in each sample, the *M*-O distances of the *M*4 sites in both samples are distinctly lower than *M*2 and *M*3. This is a clear indication that, unlike the *M*2 and *M*3 sites, the *M*4 sites contain almost no vacancies and no significant substitutions of Fe or Ti. Significant amounts of tetrahedrally-coordinated Al were only found at the *T*1 sites (0.15 *apfu*) but not at the *T*2 sites. The MgO content, ~0.7-0.8 wt%, is relatively high for "normal" dumortierite, but similar to dumortierites from the Saxonian Erzgebirge, Germany. Both dumortierite samples from the Gföhl unit contain relatively high OH contents (0.81-0.85 *pfu*), and measureable amounts of both F and BeO, with 0.05-0.06 wt% and 0.01-0.02 wt%, respectively. The compositions of these dumortierite crystals from different localities are very similar and may therefore reflect similar *PT* conditions and fluids during crystallization in these pegmatites of the same geological unit (Gföhl unit). FTIR spectroscopy reveals spectra in the 4000-3000 cm^{-1} domain that are markedly different from those of dumortierite samples of different origin. The lack of a band at 3675 cm^{-1} in the sample from Gföhl and the importance of the 3696 cm^{-1} band in both investigated dumortierite samples suggest a possible ordering of Mg and □ at the *M*1 site, in accord with the conclusions from the structure study.

Key-words: dumortierite, infra-red spectroscopy, crystal structure, chemical analyses.

Introduction

Dumortierite [~$(Al,\square)Al_6(BO_3)Si_3O_{16}(O,OH)_2$] (named for the French paleontologist, Eugene Dumortier) is the second most abundant borosilicate in pegmatites, aluminous metamorphic rocks, and metasomatic rocks, with only tourmaline in greater abundance. Dumortierite was recently described as a mineral from leucogranites (Fuchs & Visona, 1997) and as a mineral in hydrothermal systems (Foit *et al.,* 1989; Taner & Martin, 1993; Fuchs & Maury, 1995; Choo & Kim, 2002). Synthesis of dumortierite was undertaken by Werding & Schreyer (1983a, b) who later precisely determined the physical and chemical conditions (1986, 1988, 1990) of the mineral synthesis.

The understanding of the complexity of dumortierite chemistry with its non-stoichiometric cation occupancy and OH content was only possible after the first crystal structure refinements published by Golovastikov (1965) and Moore & Araki (1978). Grew (1996) offers a compilation of the chemical composition, structural details, and occurrence from minerals of the dumortierite group.

Dumortierite from the pegmatites of the Bohemian massif in Lower Austria was described from different localities (Fig. 1). Blue fibrous dumortierite [associated with

*E-mail: yves.fuchs@univ-mlv.fr

DOI: 10.1127/0935-1221/2005/0017-0173

0935-1221/0/0017-0173 $ 4.95

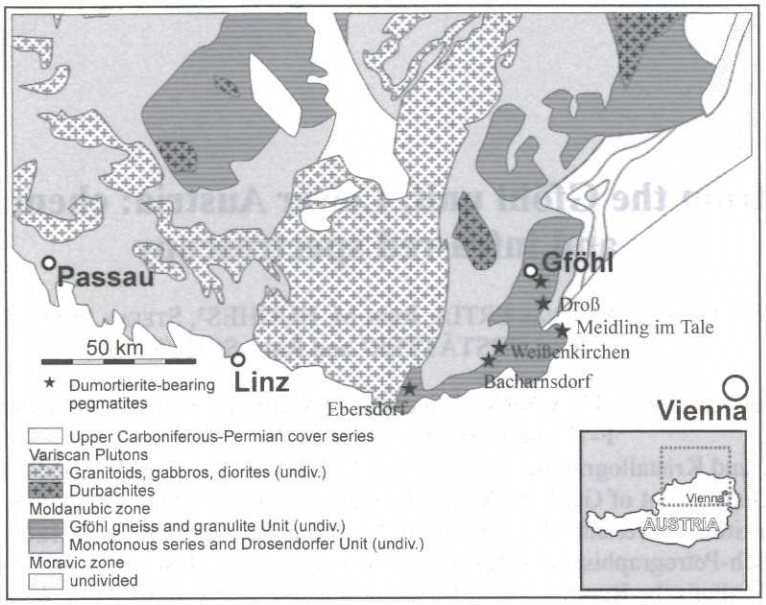

Fig. 1. Simplified geological map of the Bohemian massif with the dumortierite-bearing pegmatite localities (Gföhl unit) mentioned in the text.

schorl, dravite, olenite (Ertl *et al.,* 2001), albite, andalusite, sillimanite, almandine-spessartine, muscovite, biotite, titanite, apatite and beryl (summarized by Ertl, 1995) occurs in pegmatite veins in a quarry near the village Ebersdorf (Hlawatsch, 1911; Jobstmann, 1912). Dumortierite was also found near the village of Meidling im Tale in a large quarry. In pegmatoid veins blue-violet dumortierite (Meixner, 1952) is associated with schorl, apatite and sillimanite. Meixner (1978) described pegmatitic veins with dumortierite and apatite near the village of Bacharnsdorf. Neumayer (1980) described violet dumortierite, associated with schorl and apatite, from a quarry between the villages Lengenfeld and Droß.

One of the best dumortierite localities of Austria is a quarry south east of the village Gföhl (Fig. 1). Small pegmatite veins contain fibrous purplish grey dumortierite crystals up to 2.5 cm, which are associated with schorl, apatite, albite, orthoclase, pink to light-green fluorite, siderite, and chalcopyrite (Niedermayr, 1991). Light purple dumortierite crystals (up to 7 mm) were recently found in small pegmatite veins in a quarry (at Unterkienstock) near the village Weißenkirchen in der Wachau (Fig. 1); associated minerals are schorl, apatite, almandine-spessartine, pyrite and rutile (Kappelmüller, 1994). Here we provide detailed analyses of dumortierite crystals from Gföhl and from Weißenkirchen in der Wachau, giving infra-red spectroscopic data, chemical, and structural data. The crystals give unique IR spectra that differ from previously-reported spectra and allow conjecture of ordering in the *M1* octahedral chain.

Regional geology

The Bohemian massif is part of the deeply eroded Variscan orogen in central Europe. It is formed by the Moldanubian and the Moravian zones and by the South Bohemian Pluton. All the dumortierite-bearing pegmatites occur within the Gföhl unit of the Moldanubian zone. The Gföhl unit consists of acidic granulites, the Gföhl granite gneisses, syenite gneisses, pyroxene-bearing amphibolites, serpentinites and migmatic paragneisses (Fuchs & Matura, 1976).

For some lithologies of the Moldanubian zone a Variscan ultrahigh-pressure metamorphic imprint prior to 370 Ma is documented (peridotites of the granulite complex; Becker, 1997; Carswell, 1991), whereas the whole unit experienced a high-amphibolite- to granulite-facies overprint at about 340 Ma (~ 1000°C, 15-20 kbar; Carswell & O'Brien, 1991, 1993; Nasr & Richter, 1998). In the Gföhl unit metamorphic conditions of 700-800°C and 8-11 kbar were described (Petrakakis, 1997). During the decompression an intra-Moldanubian nappe-stack formed, which was subsequently overthrust onto the Moravian zone to the east. Major deformation is post-dated by the intrusion of the South Bohemian Pluton. The latter can be subdivided in a sequence of intrusive suites which intruded between 340 and 300 Ma (Klötzli *et al.*, 1999). In general, the pegmatites are related to the South Bohemian Pluton or to decompression melting of the metamorphic rocks. However, the origin of the dumortierite-bearing pegmatites remains unknown.

Sample selection

Fragments were separated from dumortierite crystals from Gföhl (DUM1, purplish grey, ~ 100 μm in diameter), Lower Austria, and Weißenkirchen in der Wachau (DUM2, light purple, ~ 200 μm in diameter), Lower Austria. The two crystals were first used for structure determinations and subsequently for chemical analyses. Several other frag-

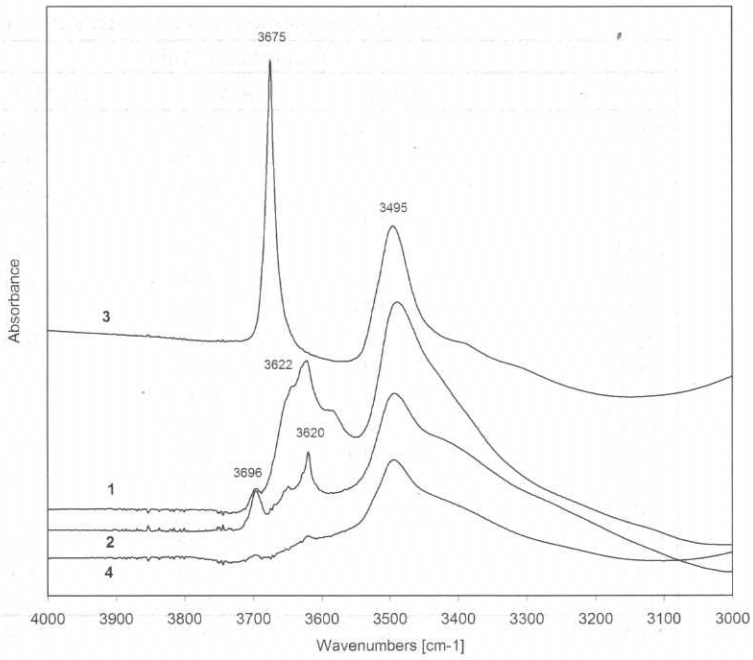

Fig. 2. FTIR spectra of dumortierite from Gföhl (1), Lower Austria, Weißenkirchen (2), Lower Austria, Lincoln Hill (3), Humboldt County, Nevada, and Saharina (4), Madagascar, in the 3000-4000 cm^{-1} region.

Table 1. Absorption bands of dumortierite in the OH stretching absorption zone.

Wavenumber [cm^{-1}]	DUM1[1]	DUM2[2]	Saharina, Madagascar	Lincoln Hill, Nevada, U.S.A.
	3494 br. m. pk.	**3493** br. m. pk.	**3494** br. m. pk.	**3495** br. m. pk.
	3585 br. sh.			
	3622 m. pk	**3620** str. pk.	3622 sh.	
		3630 w. sh.		
		3649 l. pk.		
	3653 sh.	3656 w. sh.		
		3675 sh.		**3675** str. pk.
	3697 pk.	**3696** str. pk.	3697 w. pk.	

Note: [1]From Gföhl, Lower Austria. [2]From Weißenkirchen in der Wachau, Lower Austria. pk.= peak, sh.= shoulder, br. = broad, m. = major, str. = strong, l. = little, w. = weak.
Most important peaks: **bold**

Table 2. Absorption bands of the antisymmetric B-O bonds in the BO3 triangle.

	DUM1[1]	DUM2[2]	Lincoln Hill, Nevada, U.S.A.
Wavenumber [cm^{-1}]	**1384** m. pk.	**1385** br. Pk.	1390 br
	1361 br. sh.	1363 br. Sh.	1366

Note: [1]From Gföhl, Lower Austria. [2]From Weißenkirchen in der Wachau, Lower Austria.

ments of the same dumortierite crystals were used for infrared spectroscopy.

Analytical techniques

Infra-red spectroscopy

The FTIR spectra (Fig. 2) were recorded using a Nicolet 560 ESP spectrometer. Samples were powdered and diluted in KBr at 0.5 and 1.5 % concentration, and pressed to disks. Table 1 lists the absorption bands for the dumortierites described herein as well as dumortierite from Madagascar and Nevada, U.S.A. Table 2 shows the absorption bands of the antisymmetric B-O bonds in the BO_3 triangle.

Chemistry

Two different microprobes at different laboratories were employed for analysis of these samples. Both samples were analyzed with a Cameca SX51 electron microprobe (EMP) at the Mineralogical Institute, University of Heidelberg, Germany, equipped with five wavelength-dispersive spectrometers. Operating conditions were 15 kV accelerating

Table 3. Compositions of dumortierite from the Gföhl unit, Lower Austria.

	Dumortierite, Gföhl			Dumortierite, Weißenkirchen		
	DUM1[1]	DUM1[2]	DUM1[4]	DUM2[1]	DUM2[2]	DUM2[4]
SiO_2	30.80	29.92	30.38	30.68	30.21	30.20
TiO_2	1.21	1.18	0.99	1.76	1.74	1.28
B_2O_3	-	6.36[3]	6.18	-	6.40[3]	6.18
Al_2O_3	59.01	59.54	59.97	60.29	59.22	59.84
Cr_2O_3	<0.01	0.01	-	0.01	0.01	-
FeO	0.48	0.48	0.51	0.31	0.33	0.26
MnO	0.01	0.01	-	0.01	0.01	-
MgO	0.67	0.69	0.64	0.81	0.84	0.86
CaO	0.01	0.01	-	0.01	0.01	-
Li_2O	-	<0.01[3]	-	-	<0.01[3]	-
BeO	-	0.02	-	-	0.01	-
Na_2O	0.01	0.01	-	0.01	0.01	-
K_2O	0.01	0.01	-	0.02	0.01	-
ZnO	-	0.01	-	-	0.01	-
F	-	0.06	0.07	-	0.05	0.03
H_2O	-	1.29[3]	1.29	-	1.35[3]	1.36
O=F	-	-0.03	-0.03	-	-0.02	-0.01
Sum	92.21	99.57	100.00	93.91	100.19	100.00
(O,OH)	18	18	18	18	18	18
Si	-	2.85	2.85	-	2.85	2.83
Be	-	0.00	-	-	0.00	-
B	-	1.04	1.00	-	1.04	1.00
Al	-	6.67	6.63	-	6.60	6.61
Cr	-	0.00	-	-	0.00	-
Mn^{2+}	-	0.00	-	-	0.00	-
Fe^{2+}	-	0.04	0.04	-	0.03	0.02
Mg	-	0.10	0.09	-	0.12	0.12
Zn	-	0.00	-	-	0.00	-
Ti	-	0.08	0.07	-	0.12	0.09
Li	-	0.00	-	-	0.00	-
Ca	-	0.00	-	-	0.00	-
Na	-	0.00	-	-	0.00	-
K	-	0.00	-	-	0.00	-
Sum cations	-	10.78	10.68	-	10.76	10.67
OH	-	0.82	0.81	-	0.85	0.85
F	-	0.02	0.02	-	0.01	0.01
Sum OH + F	-	0.84	0.83	-	0.86	0.86

Note: [1]Average of 10 EMP analyses (Mineralogisch-Petrographische Abteilung, Naturhistorisches Museum). P, Ni, Nb, Ta and As were not detected in any sample. [2]Average of 15 EMP analyses for DUM1 and average of 30 EMP analyses for DUM2 (Mineralogisches Institut, Universität Heidelberg). Cl was not detected in any sample. [3]Average of 2 SIMS analyses for B_2O_3 and Li_2O (3 ppm) for DUM1, average of 3 SIMS analyses for B_2O_3 and Li_2O (5 ppm) for DUM2, and one SIMS analysis for H_2O for DUM1 and average of 2 SIMS analyses for H_2O for DUM2. [4]Wt. percent calculated from optimal site occupancies and normalized to 100%. [4]B_2O_3 calculated as B = 1.00. Dash - not analyzed.

voltage, 20 nA beam current and a beam diameter of 5 μm. Peaks for all elements were measured for 10 s, except for Mg (20 s), Cr (20 s), Ti (20 s), Zn (30 s) and F (40 s). Natural and synthetic silicate and oxide standards were used for calibration. The analytical data were reduced and corrected using the PAP routine. For dumortierite, a modified matrix correction was applied assuming stoichiometric oxygen and all non-measured components to be B_2O_3. The accuracy of the electron-microprobe analyses of dumortierite and the correction procedure was checked by measuring three samples of reference tourmalines (98114: elbaite, 108796: dravite, 112566: schorl). Compositions of these tourmaline samples are presented in the interlaboratory comparison study (Dyar *et al.*, 1998, 2001). Coincidence between the published analyses and the measured values was satisfactory.

The same dumortierite samples were analyzed with a wavelength-dispersive ARL SEMQ electron microprobe at the Mineralogisch-Petrographische Abteilung, Naturhistorisches Museum, Wien, Austria. The operating

Table 4. Crystal data and results of structure refinements for dumortierite from Gföhl (DUM1), Lower Austria, and Weißenkirchen in der Wachau (DUM2), Lower Austria.

Space group: *Pnma*	
Unit cell parameters (Å):	
DUM1: a = 4.6900(3) b = 11.7875(6) c = 20.1823(11)	
DUM2: a = 4.6948(2) b = 11.8037(5) c = 20.2106(8)	
Frame width, scan time, number of frames, detector distance: 0.20°, 15 s, 4500, 5 cm	
Measured reflections, full sphere:	
DUM1: 25,929	DUM2: 25,263
Unique reflections; refined parameters:	
DUM1: 1,683; 148	DUM2: 1,697; 148
R_{int}:	
DUM1: 0.0167	DUM2: 0.0142
$R1$, $I > 4\sigma_I$:	
DUM1: 0.0181	DUM2: 0.0194
Difference peaks (+,-):	
DUM1: 0.34, 0.50	DUM2: 0.30, 0.73
Goodness-of-Fit:	
DUM1: 1.127	DUM2: 1.157

conditions were 15 kV accelerating voltage, sample current 15 nA (on benitoite), and spot size 10 µm (defocused beam). Natural silicates and oxides were used as standards.

H, Be, Li and B concentrations were determined by secondary ion mass spectrometry (SIMS) with a CAMECA ims 3f ion microprobe. Primary ions were O- ions accelerated to 10 keV. The mass spectrometer's energy window was set to 40 eV. An offset of 75 V was applied to the secondary accelerating voltage of 4.5 kV, so that secondary ions with an initial energy of 75 ± 40 eV were analysed (energy filtering). This adjustment suppresses effects of light elements related to the structure of the matrix (Ottolini *et al.,* 1993). For B, Be and Li the primary current was 20 nA, resulting in a sputtering surface of ~ 30 µm in diameter. The spectrometer's mass resolution M/ΔM for B, Be and Li was set to ~ 1100 (10 %) to suppress interferences ($6LiH^+$, $10BH^+$, Al^{3+}). Secondary ions ^7Li, ^9Be and ^{11}B were collected under an ion-imaged field of 150 µm diameter. For H the primary beam current was 20 nA and M/ΔM was set to ~ 400 (10 %). To reduce the rate of contamination with water a smaller field aperture was chosen, thus the analyzed area was restricted to 10 µm in diameter in the center of the scanned area. This method reduces the effect of water contamination, which was found to be higher on the edge of the primary beam spot than in the center. Water contamination was further reduced using a cold-trap cooled with liquid nitrogen attached to the sample chamber of the ims 3f. The count rates of the analysed isotopes (^1H, ^7Li, ^9Be and ^{11}B) were normalized to the count rate of ^{30}Si.

The relative ion yield (RIY) for B was determined using three different tourmalines as reference material: elbaite (98144), dravite (108796) and schorl (112566) described and analyzed by Dyar *et al.* (1998, 2001). For Li and Be the reference material was the SRM610 standard glass by NIST with concentrations for Li and Be published by Perkins *et al.* (1997). The relative reproducibility (1σ) for the RIY of B, Li and Be was < 1 %. Because of a substantial matrix effect during H-measurements (King *et al.,* 2002) the RIY for H was determined using only elbaite (98144) because its composition is relatively similar to the composition of the analyzed dumortierites.

Matrix effects and the uncertainty of the element concentrations in the reference material limit the accuracy. The relative uncertainty is estimated to be < 30 % for H, < 20 % for Li and < 10 % for B. Table 3 contains complete chemical analyses for crystals DUM1 and DUM2.

Crystal structure

The dumortierite crystals were mounted on a Bruker Apex CCD diffractometer equipped with graphite-monochromated Mo$K\alpha$ radiation. Redundant data were collected for an approximate sphere of reciprocal space to 60.1° 2θ, and were integrated and corrected for Lorentz and polarization factors using the Bruker program SAINTPLUS (Bruker AXS Inc. 2001). Redundancy factors of 10.92 and 10.89 were obtained for DUM1 and DUM2 respectively.

The structures were refined using dumortierite starting models and the Bruker SHELXTL V. 6.10 package of programs, with neutral-atom scattering factors and terms for anomalous dispersion. Refinement was performed with anisotropic thermal parameters for all non-hydrogen atoms. In Table 4 we list the crystal data, in Table 5 atom parameters are listed, and in Table 6 we present selected interatomic distances. Table 7 lists the anisotropic thermal parameters for atoms in the Austrian dumortierites; it is available from the authors or through the E.J.M. Editorial Office – Paris.

Results

Infra-red spectroscopy

The OH bonds stretching region

There are several published infrared spectra of dumortierite in the literature but they were rarely inter-

Table 5. Positional Parameters and equivalent isotropic displacement parameter for dumortierite from Gföhl (DUM1), Lower Austria, and Weißenkirchen in der Wachau (DUM2), Lower Austria.

DUM1:					
Atom	***x***	***y***	***Z***	***Ueq***	***Occ.***
*T*1	0.58715(10)	1/4	0.40541(2)	0.00717(15)	$Si_{0.954(3)}$
*T*2	0.91289(7)	-0.02418(3)	0.671678(16)	0.00710(11)	$Si_{0.952(2)}$
*M*1	0.6024(2)	3/4	0.74985(4)	0.0271(3)	$Al_{0.859(3)}$
*M*2	0.05807(7)	0.11044(3)	0.472510(16)	0.00578(11)	$Al_{0.950(2)}$
*M*3	0.44028(7)	0.00893(3)	0.568913(17)	0.00587(11)	$Al_{0.951(2)}$
*M*4	0.44231(8)	0.14142(3)	0.711001(17)	0.00753(12)	$Al_{0.949(2)}$
B	0.2749(4)	1/4	0.58386(9)	0.0088(3)	$B_{1.00}$
O1	0.8769(3)	1/4	0.45419(6)	0.0102(2)	$O_{1.00}$
O2	0.3375(3)	1/4	0.64938(6)	0.0110(2)	$O_{1.00}$
O3	0.39605(17)	0.13933(7)	0.42443(4)	0.00916(16)	$O_{1.00}$
O4	1.09935(17)	0.06414(7)	0.71730(4)	0.00947(16)	$O_{1.00}$
O5	1.10440(17)	-0.05002(7)	0.60651(4)	0.00905(16)	$O_{1.00}$
O6	0.61931(18)	0.04612(7)	0.64971(4)	0.01037(17)	$O_{1.00}$
O7	0.8507(2)	-0.13869(8)	0.71307(4)	0.01500(18)	$O_{1.00}$
O8	0.6511(3)	1/4	0.32635(6)	0.0151(2)	$O_{1.00}$
O9	0.24556(18)	0.14885(7)	0.55201(4)	0.00975(16)	$O_{1.00}$
O10	0.7387(3)	1/4	0.72778(6)	0.0112(2)	$O_{1.00}$
O11	-0.25017(17)	0.03358(7)	0.51196(4)	0.00821(16)	$O_{1.00}$
DUM2:					
Atom	***x***	***y***	***Z***	***Ueq***	***Occ.***
*T*1	0.58718(10)	1/4	0.40559(2)	0.00695(17)	$Si_{0.957(3)}$
*T*2	0.91298(7)	-0.02388(3)	0.671550(17)	0.00683(12)	$Si_{0.953(3)}$
*M*1	0.6045(3)	3/4	0.74985(4)	0.0277(3)	$Al_{0.853(4)}$
*M*2	0.05808(8)	0.11043(3)	0.472535(18)	0.00568(12)	$Al_{0.953(3)}$
*M*3	0.44026(8)	0.00893(3)	0.568892(18)	0.00550(12)	$Al_{0.950(3)}$
*M*4	0.44214(8)	0.14144(3)	0.710922(18)	0.00741(13)	$Al_{0.954(3)}$
B	0.2749(4)	1/4	0.58384(9)	0.0082(3)	$B_{1.00}$
O1	0.8767(3)	1/4	0.45429(6)	0.0099(2)	$O_{1.00}$
O2	0.3365(3)	1/4	0.64939(6)	0.0108(2)	$O_{1.00}$
O3	0.39593(18)	0.13930(8)	0.42450(4)	0.00874(17)	$O_{1.00}$
O4	1.09924(19)	0.06427(8)	0.71729(4)	0.00903(18)	$O_{1.00}$
O5	1.10440(18)	-0.04995(8)	0.60648(4)	0.00875(17)	$O_{1.00}$
O6	0.61918(19)	0.04632(8)	0.64962(4)	0.01006(18)	$O_{1.00}$
O7	0.8502(2)	-0.13825(8)	0.71292(5)	0.0145(2)	$O_{1.00}$
O8	0.6516(3)	1/4	0.32667(7)	0.0146(3)	$O_{1.00}$
O9	0.24548(19)	0.14892(7)	0.55200(4)	0.00951(18)	$O_{1.00}$
O10	0.7385(3)	1/4	0.72775(6)	0.0107(2)	$O_{1.00}$
O11	-0.25016(18)	0.03342(7)	0.51193(4)	0.00764(17)	$O_{1.00}$

preted. Povarennykh (1970) recognized the absorption bands at 1392 and 1362 cm^{-1} related with the ν_3 vibration of the BO_3 bond. Farmer (1974) described the vibrations related to the BO_3 and BO_4 in different boron silicates, including dumortierite, but ignored the OH bonds stretching zone. Beukes *et al.* (1987) published the IR spectrum of a Ti-rich dumortierite of South Africa. They attributed the series of low intensity absorption bands at 1390 and 3700 cm^{-1} to B-O stretching bands. They assumed that the broad band at 3450 cm^{-1} could be related to an OH-stretching mode but attributed it finally to the moisture of the KBr disc. Comparing the IR spectra of dumortierite and holtite Voloshin *et al.* (1987) identified absorption bands in dumortierite at 3690 cm^{-1}, 3615 cm^{-1}, 3500 cm^{-1} and 3400 cm^{-1}.

Assigning the absorption bands in dumortierite in the 3000-4000 cm^{-1} region is still difficult because the number of OH groups and their location are still under discussion. It is now proposed that hydroxyl groups in dumortierite substitute for O(2) and O(7) between the *M*1 octahedron and the $[SiO_4]$ tetrahedron to charge-balance the vacancies at the *M*1 site. OH groups can also balance heterovalent substitutions at the *M*1 octahedral site (Mg^{2+} and/or Fe^{2+} for Al^{3+}) or $[SiO_4]$ tetrahedral sites (Al^{3+} and/or Fe^{3+} for Si^{4+}).

Ferraris *et al.* (1995) assumed, on the basis of their crystal structure study of a high-pressure magnesiumdumortierite (Mg-rich dumortierite), that one more H could be associated to O(10) and that another (50 % occupied) H could be bound to O(9) and/or to O(1). Hence, the B-O(9) bond is probably a B-OH bond in this particular type of dumortierite.

Because our structural studies (see below) do not show evidence of these additional OH groups in the dumortierite samples from Gföhl and Weißenkirchen for our interpreta-

Table 6. Selected interatomic distances (?) for dumortierite from Gföhl (DUM1), Lower Austria, and Weißenkirchen in der Wachau (DUM2), Lower Austria.

DUM1			DUM2		
*T*1 -	O8	1.624(1)	*T*1 -	O8	1.623(2)
	O3(x2)	1.6286(9)		O3(x2)	1.6308(9)
	O1	1.678(1)		O1	1.678(1)
Mean		**1.6398**	**Mean**		**1.6407**
*T*2 -	O7	1.6138(9)	*T*2 -	O7	1.615(1)
	O5	1.6216(9)		O5	1.6224(9)
	O4	1.6421(9)		O4	1.6437(9)
	O6	1.6670(9)		O6	1.669(1)
Mean		**1.6361**	**Mean**		**1.6375**
*M*1 -	O7(x2)	1.905(1)	*M*1 -	O7(x2)	1.905(1)
	O7'(x2)	1.917(1)		O7'(x2)	1.932(1)
	O8	1.929(2)		O8	1.929(2)
	O8'	1.944(2)		O8'	1.959(2)
Mean		**1.920**	**Mean**		**1.927**
*M*2 -	O11	1.8827(9)	*M*2 -	O11	1.8853(9)
	O9	1.8849(9)		O9	1.8867(9)
	O1	1.8882(7)		O3	1.891(1)
	O3	1.8895(9)		O1	1.8908(7)
	O5	1.9055(9)		O5	1.9083(9)
	O11'	1.9473(9)		O11'	1.9481(9)
Mean		**1.8997**	**Mean**		**1.9017**
*M*3 -	O11	1.8744(9)	*M*3 -	O11	1.8766(9)
	O5	1.8815(9)		O5	1.883(1)
	O6	1.8859(9)		O6	1.8874(9)
	O3	1.9134(9)		O3	1.916(1)
	O9	1.9158(9)		O9	1.919(1)
	O11'	1.9262(9)		O11'	1.9273(9)
Mean		**1.8995**	**Mean**		**1.9016**
*M*4 -	O2	1.8510(9)	*M*4 -	O2	1.853(1)
	O4	1.8530(9)		O4	1.854(1)
	O4'	1.8618(9)		O4'	1.8652(9)
	O6	1.8658(9)		O6	1.867(1)
	O10	1.920(1)		O10	1.922(1)
	O10'	2.019(1)		O10'	2.023(1)
Mean		**1.8951**	**Mean**		**1.8974**
B -	O2	1.355(2)	**B -**	O2	1.356(2)
	O9(x2)	1.362(1)		O9(x2)	1.363(1)
Mean		**1.360**	**Mean**		**1.361**

tion of the FTIR spectra we apply the similar number and locations of the OH as in the structure model by Moore & Araki (1978).

The frequency of the OH stretching band mainly depends on the O-H bond length, which in turn is determined by the valence on the oxygen. As an application of Pauling's rules, a vacancy at the *M*1 site leads to an excess of 0.5 valence units (v. u.) on the oxygen. In contrast, the substitution of a divalent cation for Al at the *M*1 site only leads to an excess of 0.16 v.u. on the oxygen. Accordingly, the OH bond length is shorter, and the OH stretching frequency is higher, when the OH group is close to a vacancy.

Substitutions at the $^{[6]}M1$ site, where R^{2+}-elements (Mg, Fe^{2+}) can substitute for Al, result in the following environments for OH:

1. $Si^{4+}\ Al^{3+}\ R^{2+} \rightarrow$ 9-charges

The band observed at ~ 3495 cm^{-1} is attributed to the OH stretching band in the 9-charges environment accordingly to theoretical calculations (Farmer 1974, Hawthorne 1988) and compared to other silicate minerals. The width of this band, which is very important, is related to the different occupants (Mg^{2+}, Fe^{2+}, Mn^{2+}) at the *M*1 site.

2. $Si^{4+}\ R^{2+}\ R^{2+} \rightarrow$ 8-charges

The band located at ~ 3620 cm^{-1} is attributed to the stretching of OH bounds in an 8 charges environment. The existence of an 8-charges environment is related to the existence of $R^{2+} \leftrightarrow R^{2+}$ dimers in the adjacent *M*1 site. This is distinctive, as confirmed by Mössbauer and RPE spectra (Fuchs *et al.* submitted).

3. $Si^{4+}Al^{3+}\square \rightarrow$ 7-charges

Contrary to the band at ~ 3495 cm^{-1}, the width of the band at ~ 3675 cm^{-1} is relatively small in the most dumortierite samples. This suggests that normally no

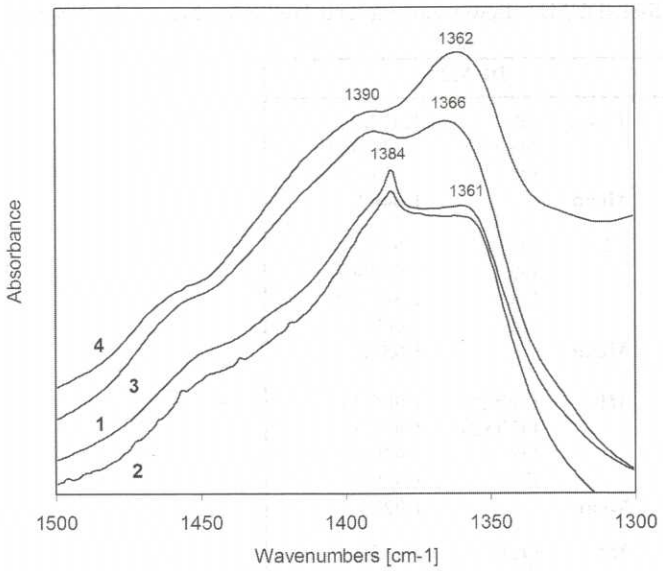

Fig. 3. FTIR spectra of dumortierite from Gföhl (1), Lower Austria, Weißenkirchen in der Wachau (2), Lower Austria, Lincoln Hill (3), Humboldt County, Nevada, and Saharina (4), Madagascar, in the 1500-1300 cm^{-1} region.

substitution occurs in the other neighbouring octahedron and tetrahedron.

Dumortierite samples of different origin show important variations of their FTIR spectra. In the dumortierite samples of this study two major bands, at 3495 cm^{-1} (substitution for Al at the *M*1 site by a R^{2+} cation) and 3675 cm^{-1} (vacancy at the *M*1 site), characterize the 4000-3000 cm^{-1} domain. The presence of divalent dimers in two adjacent *M*1 sites, and substitutions at the adjacent Si^{4+} tetrahedron result in an increasing complexity of the dumortierite FTIR spectra.

Dumortierite FTIR spectra (Fig. 2) from samples from the Gföhl unit (1 and 2) are relatively complicated compared to those from Lincoln Hill (Nevada, USA) (3) and Madagascar (Saharina) (4). Numerous absorption bands are present in the 4000-3000 cm^{-1} region in dumortierite samples from the Gföhl unit. Important absorption peaks at ~ 3495 and at ~ 3620 cm^{-1} suggest that the most frequent cationic arrangements neighbouring the hydroxyl group are one of the following types:

- Si^{4+} Al^{3+} R^{2+} → 9-charges
- Si^{4+} R^{2+} R^{2+} → 8-charges

Saharina sample (4) (Fig. 2) shows a strong absorption band at 3495 cm^{-1}, revealing the preeminence of Al cations in the environment of the hydroxyl group, an interpretation consistent with the crystal chemistry of this sample. Lincoln Hill sample (3) (Fig. 2) with two peaks at 3495 and 3675 cm^{-1} shows a representative FTIR spectra for many dumortierites in which the OH shows 9-charges environments and 7-charges environments, a site occupation that is consistent with the EPR, and XANES spectroscopy of this sample (Fuchs *et al.,* 2004 and submitted).

The FTIR spectra of the Gföhl and Weissenkirchen dumortierite samples are more complicated. The presence of numerous peaks between 3650 and 3700 cm^{-1} suggests different environments for the hydroxyl group when the *M*1 site is vacant. Possible substitutions of trivalent cations (Al^{3+}, Fe^{3+}) or fourvalent cations (Ti^{4+}) in the tetrahedron are:

e.g., $(Al^{3+}, Fe^{3+})^{[4]}(Ti^{4+})^{[6]}\square^{[6]}$ or $(Si^{4+},Ti^{4+})^{[4]}(Al^{3+}, Fe^{3+})^{[6]}\square^{[6]}$.

Such a situation differs from that of the Lincoln Hill sample (Fig. 2), where the 3675 cm^{-1} band is well characterized with a narrow width, which is attributed to the strong ordering and the lack of substitutions at the neighbouring sites (Fuchs *et al.,* 2004 and submitted). As will be shown subsequently, these characteristics of the dumortierites from the Gföhl unit are consistent with the site occupancies optimized from the structural and chemical data.

The 1500-1300 domain (B-O bonds)

In the dumortierite structure two B-O bonds are linked with an *M*2-*M*3 double edge-sharing chain and one *M*4 face sharing chain. This particular disposition is probably responsible for the existence of two peaks in this domain (Fig. 3). The Lincoln Hill (3; Fig. 3) and the Saharina dumortierite (4; Fig. 3) spectra also show a double absorption peak, but the position of these peaks is shifted and the relative intensity is different, reflecting the different occupation of the *M*4 site in these samples (Fuchs *et al.,* 2004 and submitted).

Crystal structure

Moore & Araki (1978) offered a detailed structure analysis of dumortierite. We refer the reader to their work for structural principles for dumortierite, and here provide structural details derived from the Austrian dumortierites, particularly regarding the *M*1 octahedral chains.

The principal structure aspect of interest in dumortierite is the chain formed of face-sharing octahedra, the $\infty[M1O_3]$ chain. Moore (1973) proffered a geometric analysis of such chains in his study of "bracelet and pinwheel" structures based on hexagonal closest-packed oxygen atoms. In dumortierite, the central octahedral chain is the $\infty[M1O_3]$ chain formed of face-sharing octahedra. Each apex of the octahedron is decorated with a tetrahedron, which together with the octahedron form the geometric pinwheel common in many hexagonal closest-packed oxygen arrays. In the central octahedral chain the Al atoms in the face-centered octahedra are unusually close; in DUM1, adjacent Al atoms are 2.3450(1) Å distant, and in DUM2 they are separated by 2.3474(1) Å. Moore & Araki (1978) noted that the octahedral centers in the *M*1 chain were approximately $^3/_4$ occupied, and suggested that the chains exist as trimers of Al-centered octahedra, in a sequence of □ – Al – Al –Al – □. Those authors suggest that with disorder in the *M*1 octahedral chain, the average chain length can be adjusted to fit the remaining octahedral framework in the structure. They also note that although the existence of face-sharing trimers is well-known in octahedral chains, longer chain segments have not been observed in ionic compounds. In the Austrian dumortierites, the chain segments are indeed longer than trimers. However,

Table 8. Optimized site-occupancies (Wright et al., 2000) in Austrian dumortierites.

	DUM1:	DUM2:
*M*1:	$Al_{0.78}Ti_{0.01}Mg_{0.09}\square_{0.12}$	$Al_{0.74}Ti_{0.01}Mg_{0.12}\square_{0.13}$
*M*2:	$Al_{0.93}Ti_{0.03}\square_{0.04}$	$Al_{0.94}Ti_{0.01}Fe_{0.01}\square_{0.04}$
*M*3:	$Al_{0.94}Fe_{0.02}\square_{0.04}$	$Al_{0.93}Ti_{0.03}\square_{0.04}$
*M*4:	$Al_{0.98}\square_{0.02}$	$Al_{0.98}\square_{0.02}$
*T*1:	$Si_{0.85}Al_{0.15}$	$Si_{0.85}Al_{0.15}$
*T*2:	$Si_{1.00}Si_{0.99}Al_{0.01}$	

Note: DUM1: Gföhl, Lower Austria. DUM2: Weißenkirchen in der Wachau, Lower Austria.

the existence of significant divalent ions in the Austrian minerals, where ~ 7/8 of the octahedra are occupied in the *M*1 chain, may mitigate the need for shorter sequences.

In a bracelet and pinwheel structure with structure units isostructural with those in dumortierite, the mineral lyonsite $[Cu_3^{2+}Fe_4^{3+}(VO_4)_3^{3-}]$ also shows significant disorder and vacancies in the octahedral chains. Hughes *et al.* (1987) noted that in such chains the observed occupancies represents a space average of disordered occupied octahedra within the chains, and at higher temperatures dynamic disorder may occur at the octahedral centers in the chains. Clearly, the anisotropic thermal parameters (Table 7) show significant elongation of the electron ellipse along *a*, permissive of dynamic disorder in the *M*1 octahedral chains in dumortierite [DUM1: $u_{11} = 0.0662(6)$, $u_{22} = 0.0074(3)$, $u_{33} = 0.0077(3)$; DUM2: $u_{11} = 0.0682(7)$, $u_{22} = 0.0072(3)$, $u_{33} = 0.0076(3)$].

Wright *et al.* (2000) offered a method for using structure and chemistry data to optimize the site-occupancies of complex minerals. Applying quadratic programming methods to the data for the Austrian dumortierites, the occupancies of *M*1-*M*4, *T*1 and *T*2, are obtained (Table 8). Those occupancies support earlier findings that the majority of octahedral substituents locate at *M*1. Moore & Araki (1978) also released the occupants of the octahedral sites in their refinement, and obtained similar results to those reported herein. Because of the high quality of the structure refinements of our dumortierite samples (R = 0.018-0.019), the *M*-O distances are very accurate (Table 6). Although the average *M*-O distances of the *M*2 and *M*3 sites are similar in each sample, the *M*-O distances of the *M*4 sites are distinctly lower (0.004-0.005 Å, Table 6). Because the effective ionic radii (6-coordination) of Fe^{2+}, Fe^{3+}, Ti^{3+} and Ti^{4+} are larger than those of Al, such short *M*-O distances are a clear indication that, unlike the *M*2 and *M*3 sites, the *M*4 sites contain almost no vacancies and no significant substitutions of Fe or Ti (Table 8). The optimized formulae in conventional dumortierite format and considering the site occupants given in Table 8, for dumortierite from Gföhl (DUM1), Lower Austria, and for dumortierite from Weißenkirchen in der Wachau (DUM2), Lower Austria, are:

DUM1: $(Al_{0.78}\square_{0.12}Mg_{0.09}Ti_{0.01})$ $(Al_{5.70}\square_{0.20}Ti_{0.06}Fe_{0.04})$ $(Si_{2.85}Al_{0.15})$ B O_{16} $[O_{1.17}(OH)_{0.81}F_{0.02}]$

DUM2: $(Al_{0.74}\square_{0.13}Mg_{0.12}Ti_{0.01})$ $(Al_{5.70}\square_{0.20}Ti_{0.08}Fe_{0.02})$ $(Si_{2.83}Al_{0.17})$ B O_{16} $[O_{1.14}(OH)_{0.85}F_{0.01}]$

Discussion

FTIR spectroscopy of the Gföhl dumortierite samples were studied in two domains: the 3800-3200 cm^{-1} and the 1300-1500 cm^{-1} domain.

3800-3200 cm^{-1} domain

The 3800-3200 cm^{-1} domain contains the stretching bonds of the OH groups. As OH groups replace O2 and O7 and are located between one Si tetrahedron and 2 *M*1 octahedra the localization of the absorption bands reflects the substitutions occurring in the *M*1 site and in the tetrahedron. Clearly the band at ~ 3495 cm^{-1} represents the most frequent 9-charges environment $^{(T)}R^{4+},^{(M1)}R^{3+},^{(M1)}R^{2+}$ or $^{(T)}R^{3+},^{(M1)}R^{3+},^{(M1)}R^{3+}$. Usually it is a broad major band in dumortierite. The band at ~ 3620 cm^{-1} (8-charges) represents an 8-charges environment $^{(T)}Si^{4+},^{(M1)}R^{2+}$ $^{(M1)}R^{2+}$. It is well represented in the Gföhl dumortierite, weak in the Madagascar sample and non-existant in the Lincoln Hill sample. In relation to the chemistry of the Gföhl samples it seems that the divalent cation is probably Mg. The 3675 cm^{-1} band, frequent in most dumortierite samples (see Lincoln Hill) is surprisingly weak in sample 2 and totally absent in sample 1. It represents the $^{(T)}Si^{4+}$ $^{(M11)}Al^{3+}$, $^{(M1)}\square$ environment. The importance of ~ 3696 cm^{-1} peak, particularly in DUM2 could be reported to a $^{(T)}Si^{4+}$ $^{(M11)}Mg^{2+}$, $^{(M1)}\square$ environment and an ordering of Mg and $\square$.

The high number of small peaks and shoulders in sample1 and particularly sample 2 bespeaks complex substitution processes both at the *M*1 octahedron and in the tetrahedron, whereas substitutions at the *M*2, *M*3 and especially at the *M*4 sites seem to be very limited. This distribution is different from those found for some Fe-bearing dumortierite samples (Fuchs *et al.*, 2004 and submitted). *Ab initio* XANES (using FEFF) calculations at the Fe K-edge suggest that Fe is located mainly at the *M*2, *M*3 and possibly minor amounts at the *M*4 sites (having the highest energy and shorter average Al-O distances), as continued by our optimization calculations. A temperature dependence of the distortion of the different sites could explain this apparent discrepancy.

1500-1300 cm^{-1} domain:

As two B-O bonds are linked with an *M*2-*M*3 double edge-sharing chain and one with a *M*4 face-sharing chain, there would normally be two antisymmetric stretching

absorption bands, representing the two different B-O interatomic distances for B-O(9) and B-O(2) (see Table 6). Possible small vacancies at *M*2, *M*3 and *M*4, and limited substitutions of Al by Ti and Fe at *M*2 and *M*3 octahedral sites are responsible for the complexity of the resulting absorption bands.

Both investigated dumortierite crystals have very similar compositions and may therefore reflect similar *PT* conditions and fluids during crystallization in these pegmatites of the same geological unit (Gföhl unit). The MgO content is relatively high for "normal" dumortierite. MgO is ~ 0.7 wt% for dumortierite from Gföhl, and ~ 0.8 wt% for dumortierite from Weißenkirchen in der Wachau (Table 3). Similar MgO contents have been found in dumortierite samples from the Saxonian Erzgebirge, Germany (Groat *et al.,* in prep.). Magnesiodumortierite (a "high-pressure mineral") from the Dora Maira Massif, Western Alps, contains up to ~ 5.8-8.7 wt% MgO (Schertl *et al.,* 1991; Chopin *et al.,* 1995). FeO content is ~ 0.3-0.5 wt% and TiO_2 ~ 1.2-1.7 wt% in these dumortierite samples from the Gföhl unit. Both dumortierite samples from the Gföhl unit show relatively high OH contents (0.81-0.85 *pfu*) and relatively high MgO contents (~ 0.7-0.8 wt%). Elevated Mg content is associated with high OH content; the water content of magnesiodumortierite probably reaches 2 OH *pfu* (Grew, 1996). Relative to the 0.05 OH *pfu* for a dumortierite with 0.03 wt% MgO (Willner & Schreyer 1991), the elevated OH values of dumorterite from the Gföhl unit seem reasonable. Furthermore, the dumortierites from the Gföhl unit contain significant amounts of both F (0.05-0.06 wt%) and BeO (0.01-0.02 wt%). These are the highest BeO contents that have been measured in dumortierite to date. Dumortierite samples with relatively high concentrations of As, Ta, Nb, Sb and Bi are described in an extensive study by Groat *et al.* (in prep.).

Acknowledgements: We are grateful to A. Wagner, Vienna, Austria, for the excellent preparation of the dumortierite samples for analysis. Special thanks to L.A. Groat and E.S. Grew for information about the chemical compositions of their studied dumortierite samples and to George R. Rossman for helpful comments. Sincere thanks are expressed to C. Paulmann and to two anonymous reviewers for their comments on this work. This work was supported, in part, by NSF grants EAR-9627222, EAR-9804768, and EAR-0003201 to JMH.

References:

Becker, H. (1997): Petrological constraints on the cooling history of high-temperature garnet peridotite massifs in lower Austria. *Contrib. Mineral. Petrol.*, **92**, 448-455.

Beukes, G.J., Slabbert, M.J., de Bruiyn, H., Botha, B.J.V., Schoch, A.E. (1987): Ti dumortierite from Keimoes area, Namaqua mobile belt, South Africa. *N. Jb. Miner. Abh.*, **157**, 303-318.

Carswell, D.A. (1991): Variscan high P-T metamorphism and uplift history in the Moldanubian Zone of the Bohemian Massif in Lower Austria. *Eur. J. Mineral.*, **3**, 323-342.

Carswell, D.A. & O'Brien, P.J. (1991): High pressure granulites in the Moldanubian zone, Lower Austria. *Terra Abstr.*, **31**, 93.

—,— (1993): Thermobarometry and geotectonic significance of high-pressure granulite examples from the Moldanubian Zone of the Bohemian Massif in Lower Austria. *J. Petrol.*, **34**, 427-459.

Choo, C.O. & Kim, Y. (2002): SEM, FTIR, and NMR studies of dumortierite from an Al-rich clay deposit, Korea. 12th Annual V.M. Goldschmidt Conference, Davos, Switzerland, 140.

Chopin, C., Ferraris, G., Ivaldi, G., Schertl, H.P., Schreyer, W., Compagnoni, R., Davidson, C., Davis, M., A. (1995): Magnesiodumortierite, a new mineral from very-high-pressure rocks (western Alps), II Crystal chemistry and petrological significance. *Eur. J. Mineral.*, **7**, 525-535.

Dyar, M.D., Taylor, M.E., Lutz, T.M., Francis, C.A., Guidotti, C.V., Wise, M. (1998): Inclusive chemical characterization of tourmaline: Mössbauer study of Fe valence and site occupancy. *Am. Mineral.*, **83**, 848-864.

Dyar, M.D., Wiedenbeck, M., Robertson, D., Cross, LR., Delaney, J.S., Ferguson, K., Francis, C.A., Grew, E.S., Guidotti, C.V., Hervig, R.L., Hughes, J.M., Husler, J., Leeman, W., McGuire, A.V., Rhede, D., Rothe, H., Paul, R.L., Richards, I., Yates, M. (2001): Reference Minerals for the Microanalysis of Light Elements. *Geostand. Newsl.*, **25**, 441-463.

Ertl, A. (1995): Elbait, Olenit, Dravit-Buergerit-Mischkristalle, Dravit, Uvit und ein neuer Al-Turmalin (?) von österreichischen Fundstellen. *Mitt. Österr. Miner. Ges.*, **140**, 55-72.

Ertl, A., Pertlik, F., Bernhardt, H.-J. (2001): Hellblaue Olenit-Schörl-Dravit Mischkristalle von Ebersdorf, Niederösterreich: Chemismus und Kristallstruktur. *Mitt. Österr. Miner. Ges.*, **146**, 75-77.

Farmer, V.C. (1974): The infrared spectra of minerals. Mineralogical Society, Monograph 4, London, 539p.

Ferraris, G., Ivaldi, G., Chopin, C. (1995): Magnesiumdumortierite, a new mineral from very-high-pressure rocks (Western Alps). Part I: Crystal structure. *Eur. J. Mineral.*, **7**, 167-174.

Foit, F.F. Jr, Fuchs, Y., Myers, P.E. (1989): Chemistry of alkali-deficient schorls from two tourmaline-dumortierite deposits. *Am. Mineral.*, **74**, 1317-1324.

Fuchs, G. & Matura, A. (1976): Zur Geologie des Kristallins der Böhmischen Masse. *Jb. Geol. B.-A.*, **119/1**, 1-43.

Fuchs, Y. & Maury, R. (1995): Borosilicate alteration associated with U-Mo-Zn and Ag-Au-Zn deposits in volcanic rocks. *Mineral. Deposita*, **30**, 449-459.

Fuchs, Y. & Visona, D. (1997): Dumortierite a new mineral from Himalayan leucogranites: petrological and geochemical implications. 2nd Intern. Symp. on granites and associated mineralizations, Salvador, Bahia, 24-29/8/97. *in* extended abstracts and program, 247-248.

Fuchs, Y., Balan, E., Farges, F., Linarès, J., and Horn, A. (2004): Fe and Ti site occupation in dumortierite. A FTIR, EPR, Mössbauer and Fe/Ti K-edge XANES study. EMPG X, Francfort, Germany, 4-7/4/2004, Abstract. *Lithos*, **73**, 1-2,39.

Golovastikov, N.I. (1965): The crystal structure of dumortierite. *Doklady Akad. Nauk. SSSR*, **162**, 6, 1282-1284 (in Russian, English trans., *Sov. Phys. Doklady*, **10**, 493-495).

Grew, E.S. (1996): Borosilicates (exclusive of tourmaline) and boron in rock-forming minerals in metamorphic environments. *In*: Grew, E.S. & Anovitz, L.M. (eds.): «Boron: Mineralogy, Petrology and Geochemistry». *Rev. in Mineral.*, **33**, 387-502.

Hawthorne, F.C. (ed.) (1988): «Spectroscopic methods in mineralogy and geology». *Rev. in Mineral.*, **18**, 698 pp.

Hlawatsch, C. (1911): Über einige Mineralien der Pegmatitgänge im Gneise von Ebersdorf bei Pöchlarn, Niederösterreich. *Verh. Geol. Reichsanstalt*, **11**, 259.

Hughes, J.M., Starkey, S.J., Malinconico, M.L., Malinconico, L.L. (1987): Lyonsite, $Cu_3^{2+}Fe_4^{3+}(VO_4)_6^{3-}$, a new fumarolic sublimate from Izalco volcano, El Salvador: Descriptive mineralogy and crystal structure. *Am. Mineral.*, **72**, 1000-1005.

Jobstmann, B. (1912): Auffindung von Dumortierit im anstehenden Pegmatit bei Ebersdorf (bei Pöchlarn). *Tscherm. Mineral. Petrogr. Mitt.*, **1912**, 120.

Kappelmüller, H. (1994): Mineralfundstellen in Niederösterreich. 72 pp., Bode Verlag, Haltern, Germany.

King, P.L.,Vennenmann, T.W., Holloway, J.R., Hervig, R.L., Lowenstern, J.B., Forneris, J.F. (2002): Analytical techniques for volatiles: A case study using intermediate (andesitic) glasses. *Am. Mineral.*, **87**, 1077-1089.

Klötzli, U., Frank, W., Scharbert, S., Thöni, M. (1999): Evolution of the SE Bohemian Massif based on geochronological data – A review. *Jb. Geol. B.-A.*, **141/4**, 377-394.

Meixner, H. (1952): Neue Mineralfunde aus Österreich XII. 113. Dumortierit von Göttweig, Niederösterreich. *Carinthia II*, **142**, 38.

Meixner, H. (1978): Neue Mineralfunde aus Österreich XXVIII. *Carinthia II*, **168/88**, 81-103.

Moore, P.B. (1973) Bracelets and pinwheels: A topological-geometrical approach to the calcium orthosilicate and alkali sulphate structures. *Am. Mineral.*, **58**, 32-42.

Moore, P.B. & Araki, T. (1978): Dumortierite, $Si_3B[Al_{6.75}\square_{0.25}O_{17.25}(OH)_{0.75}]$: a detailed structure analysis. *N. Jb. Miner. Abh.*, **132**, 231-241.

Nasr, T.Y. & Richter, W. (1998): Raabser Serie: Petrologie und Geochemie der Amphibolite und Orthogneise. *Mitt. Österr. Miner. Ges.*, **143**, 349-350.

Neumayer, R. (1980): Neue Mineralfunde aus dem Waldviertel. *Mitt. Österr. Miner. Ges.*, **127**, 30-32.

Niedermayr, G. (1991): 839. Chalkopyrit, Dumortierit, Fluorit und Siderit aus einem Steinbruch südöstlich Gföhl, Niederösterreich. *In*: Niedermayr, G., Brandstätter, F., Moser, B., Postl, W., Taucher, J. (1991): Neue Mineralfunde aus Österreich XL. *Carinthia II*, **181/101**, 167.

Ottolini, L., Bottazzi, P., Vannucci, R. (1993): Quantification of lithium, beryllium, and boron in silicates by secondary Ion Mass Spectrometry using conventional energy filtering. *Analyt. Chem.*, **65**, 1960-1968.

Perkins, W.T., Pearce, N.J.G., Westgate, J.A. (1997): The development of laserablation ICP-Ms and calibration strategies; examples from the analyses of trace elements in volcanic glass shards and sulfide minerals. *Geostand. Newsl.*, **21**, 115-144.

Petrakakis, K. (1997): Evolution of Moldanubian rocks in Austria: review and synthesis. *J. metamorphic Geol.*, **15**, 203-222.

Povarennykh, A.S. (1970): Spectres infrarouges de certains minéraux de Madagascar. *Bull. Soc. Fr. Minéral. Cristallogr.*, **93**, 224-234.

Schertl, H.-P., Schreyer, W., Chopin, C. (1991): The pyrope-coesite rocks and their country rocks at Parigi, Dora Maira Massif, Western Alps: detailed petrography, mineral chemistry and PT-path. *Contrib. Mineral. Petrol.*, **108**, 1-21.

Taner, M.F. & Martin, R.F. (1993): Significance of dumortierite in an aluminosilicate-rich alteration zone, Louvicourt, Québec. *Can. Mineral.*, **31**, 137-146.

Voloshin, A.V., Pakhomovskiy, Ya.A., Zalkind, O.A. (1987): An investigation of the chemical composition and IR-spectroscopy of holtite. *Mineral'nyye Assotsiatsii i Mineraly Magmacheskikh Kompleksov Kol'skogo Polyostrova, Apatity, Kol'skiy Filial AN SSSR*, **1987**, 14-34 (in Russian).

Werding, G. & Schreyer, W. (1983a): Synthesis, crystal chemistry, and preliminary stability of dumortierite in the system SiO_2-Al_2O_3-B_2O_3-H_2O. *Forts. Mineral.*, **61**, Beiheft 1, 219-220.

—,— (1983b): High pressure synthesis of dumortierite. *Terra Cognita*, **3**, 165, 1.

—, — (1986): Dumortierite compositional variations as a function of fluid pressure and temperature. International Symposium of Experimental Mineralogy Geochemistry, Nancy, 143-144 (abstract).

—,— (1988): Synthetic dumortierites: Their PTX-dependent compositional variations in the system Al_2O_3-SiO_2-B_2O_3-H_2O. *Forts. Mineral.*, **66**, Beiheft 1, 168.

—,— (1990): Synthetic dumortierite: its PTX-dependent compositional variations in the system Al_2O_3-SiO_2-B_2O_3-H_2O. *Contrib. Mineral. Petrol.*, **105**, 11-24.

Willner, A.P. & Schreyer, W. (1991): A dumortierite-topaz-white mica fels from the peraluminous metamorphic suite of Bushmanland (South Africa). *N. Jb. Miner. Mh.*, **1991**, 223-240.

Wright, S.E., Foley, J.A., Hughes, J.M. (2000): Optimization of site occupancies in minerals using quadratic programming. *Am. Mineral.*, **85**, 524-531.

Received 5 April 2004
Modified version received 21 September 2004
Accepted 3 November 2004